

Observational signatures of the surviving donor star in the double detonation model of Type Ia supernovae

Zheng-Wei Liu^{1,2,3}, Friedrich K. Röpké^{4,5}, Yaotian Zeng^{1,2,3}, and Alexander Heger^{6,7,8,9}

¹ Yunnan Observatories, Chinese Academy of Sciences, 396 Yangfangwang, Guandu District, Kunming 650216, P.R. China
e-mail: zwliu@ynao.ac.cn

² Key Laboratory for the Structure and Evolution of Celestial Objects, CAS, Kunming 650216, P.R. China

³ University of Chinese Academy of Science, Beijing 100012, P.R. China

⁴ Zentrum für Astronomie der Universität Heidelberg, Institut für Theoretische Astrophysik, Philosophenweg 12, 69120 Heidelberg, Germany

⁵ Heidelberger Institut für Theoretische Studien, Schloss-Wolfsbrunnenweg 35, 69118 Heidelberg, Germany

⁶ School of Physics and Astronomy, Monash University, 19 Rainforest Walk, VIC 3800, Australia

⁷ Australian Research Council Centre of Excellence for Gravitational Wave Discovery (OzGrav), Clayton, VIC 3800, Australia

⁸ Center of Excellence for Astrophysics in Three Dimensions (ASTRO-3D), Stromlo, ACT 2611, Australia

⁹ Joint Institute for Nuclear Astrophysics, National Superconducting Cyclotron Laboratory, Michigan State University, 1 Cyclotron Laboratory, East Lansing, MI 48824-1321, USA

September 22, 2021

ABSTRACT

The sub-Chandrasekhar mass double-detonation (DDet) scenario is a contemporary model for Type Ia supernovae (SNe Ia). The donor star in the DDet scenario is expected to survive the explosion and to be ejected at the high orbital velocity of a compact binary system. For the first time, we consistently perform three-dimensional (3D) hydrodynamical simulations of the interaction of SN ejecta with a helium (He) star companion within the DDet scenario. We map the outcomes of 3D impact simulations into one-dimensional stellar evolution codes and follow the long-term evolution of the surviving He-star companions. Our main goal is to provide the post-impact observable signatures of surviving He-star companions of DDet SNe Ia, which will support the search for such companions in future observations. Such surviving companions are ejected with high velocities of up to about 930 km s^{-1} . We find that our surviving He-star companions become significantly overluminous for about 10^6 yr during the thermal re-equilibration phase. After the star re-establishes thermal equilibrium, its observational properties are not sensitive to the details of the ejecta-donor interaction. We apply our results to hypervelocity star US 708, which is the fastest unbound star in our Galaxy, travelling with a velocity of about $1,200 \text{ km s}^{-1}$, making it natural candidate for an ejected donor remnant of a DDet SN Ia. We find that a He-star donor with an initial mass of $\geq 0.5 M_{\odot}$ is needed to explain the observed properties of US 708. Based on our detailed binary evolution calculations, however, the progenitor system with such a massive He-star donor cannot get close enough at the moment of SN explosion to explain the high velocity of US 708. Instead, if US 708 is indeed the surviving He-star donor of a DDet SN Ia, it would require the entire pre-SN progenitor binary to travel at a velocity of about 400 km s^{-1} . It could, for example, have been ejected from a globular cluster in the direction of the current motion of the surviving donor star.

Key words. stars: supernovae: general – binaries: close

1. INTRODUCTION

It is generally accepted that Type Ia supernovae (SNe Ia) result from thermonuclear explosions of white dwarfs (WDs) in interacting binary systems. SNe Ia have been used as accurate cosmic distance indicators, which led to the discovery of the accelerating expansion of the Universe (Riess et al. 1998; Schmidt et al. 1998; Perlmutter et al. 1999). The specific progenitor systems of SNe Ia and their explosion mechanism, however, remain an unsolved problem. Different progenitor scenarios have been proposed for explaining SNe Ia (Hillebrandt et al. 2013; Maoz et al. 2014).

The sub-Chandrasekhar mass double-detonation (DDet) scenario is a promising model to explain normal SNe Ia (e.g., Shen et al. 2018; Townsley et al. 2019; Gronow et al. 2020, 2021). In this scenario, a WD accretes material from its He-rich companion star, which could be a He-burning star or a He WD, to accumulate a He layer on its surface. If the He shell

reaches a critical mass, $\approx 0.02\text{--}0.2 M_{\odot}$ (Woosley & Kasen 2011; Neunteufel et al. 2016; Polin et al. 2019), it triggers an initial detonation that ignites a second detonation of the core material. The entire sub-Chandrasekhar mass WD then undergoes a thermonuclear explosion (e.g., Taam 1980; Woosley et al. 1986; Livne & Arnett 1995; Fink et al. 2007, 2010; Sim et al. 2010; Moll & Woosley 2013; Gronow et al. 2020, 2021; Boos et al. 2021). The DDet scenario has recently gained attention because of its attractive features in explaining current observations for SNe Ia. For instance, the lack of H emission in SN Ia spectra (Leonard 2007) and the non-detection of a pre-explosion companion in HST imaging (Li et al. 2011) are inherent to DDet models. Early UV flash signatures of ejecta interaction with a companion (Kasen 2010) should be very small in the DDet scenario because binary systems are generally very close at the moment of SN explosions. In addition, population synthesis calculations show that the DDet scenario can explain a large frac-

tion of SNe Ia as well as their delay time distribution (DTD, [Ruiter et al. 2011, 2014](#)).

Observations of several binary systems composed of a WD and a He-rich companion star, e.g., KPD 1930+2752, V445 Pup, HD 49798 and CD-30°11223 systems ([Maxted et al. 2000](#); [Geier et al. 2007](#); [Kato & Hachisu 2003](#); [Kudritzki & Simon 1978](#); [Vennes et al. 2012](#); [Geier et al. 2013](#)) seem to support this scenario. For instance, CD-30°11223 is a WD + sdB star system with a WD mass of $M_{\text{WD}} = 0.76 M_{\odot}$, a companion mass of $M_{\text{sdB}} = 0.51 M_{\odot}$, and a short orbital period of $P_{\text{orb}} \simeq 1.2$ hours. [Vennes et al. \(2012\)](#) and [Geier et al. \(2013\)](#) suggest that CD-30°11223 will likely explode as a SN Ia via the DDet scenario during its future evolution.

In the DDet scenario, the companion star is expected to be significantly shocked and heated while parts of its outer layers are removed during the ejecta-companion interaction. The binary system is disrupted, but the companion star survives the interaction with the supernova blast wave and is ejected at high speed that is dominated by its pre-explosion orbital velocity (e.g., [Wheeler et al. 1975](#); [Fryxell & Arnett 1981](#); [Livne et al. 1992](#); [Marietta et al. 2000](#); [Pakmor et al. 2008](#); [Liu et al. 2012, 2013b,c,a](#); [Pan et al. 2012b](#); [Bauer et al. 2019](#); [Zeng et al. 2020](#)). Binary progenitor systems in the DDet scenario are relatively close when SN Ia explosions go off. In this scenario, the companion stars are expected to have a high orbital velocity of up to $\simeq 900 \text{ km s}^{-1}$ at the moment of explosion (e.g., [Geier et al. 2015](#); [Neunteufel 2020](#)). The surviving companion stars from this scenario are therefore good candidates of hypervelocity stars such as US 708 (e.g., [Geier et al. 2013, 2015](#); [Neunteufel 2020](#); [Neunteufel et al. 2021](#)). An unambiguous identification of a donor remnant of such an event would therefore support the DDet scenario of SNe Ia. Such an identification requires knowledge of the observable signatures of surviving companion stars of SNe Ia in the DDet scenario.

Hypervelocity stars (HVSs) are generally defined as stars that move sufficiently fast to escape the gravitational potential of our Galaxy, i.e., they typically have velocities larger than $\sim 400 \text{ km s}^{-1}$ in the Galactic rest frame (for a review see [Brown 2015](#)). HVSs are believed to be ejected by three-body interactions with the supermassive black hole at the Galactic center (e.g., [Hills 1988](#); [Yu & Tremaine 2003](#); [Brown et al. 2005](#)), exchange encounters in other dense stellar environments (e.g., [Aarseth 1974](#)) between hard binaries and massive stars (e.g., [Leonard 1991](#); [Gvaramadze et al. 2009](#)), or disruptions of close binaries via SN explosions (e.g., [Blaauw 1961](#); [Tauris & Takens 1998](#); [Zubovas et al. 2013](#); [Tauris 2015](#); [Geier et al. 2015](#); [Neunteufel et al. 2021](#)).

The hypervelocity star US 708 has been classified as a sdO/B star. Based on a spectroscopic and kinematic analysis, [Geier et al. \(2015\)](#) have reported that US 708 travels with a velocity of about $1,200 \text{ km s}^{-1}$, suggesting that it is one of the fastest unbound stars in our Galaxy that was ejected from the Galactic disc 14.0 ± 3.1 Myr ago. Considering the possibilities of different acceleration mechanisms of HVSs, [Geier et al. \(2015\)](#) further concluded that US 708 is very unlikely to originate from the Galactic center, but it is rather the ejected donor remnant of a DDet SN Ia.

[Geier et al. \(2015\)](#), however, did not compare the long-term evolution and appearance of surviving companion stars of DDet SNe Ia with the observations of US 708. It is therefore still an open question whether the observations of this star match the expected properties of a surviving SN Ia donor star in the DDet scenario. The present paper predicts observable signatures of the surviving companion stars of sub-Chandrasekhar

mass double-detonation SNe Ia by combining the outcomes of three-dimensional (3D) hydrodynamic simulations of ejecta-companion interaction with detailed one-dimensional (1D) calculations of the long-term evolution of the donor remnant. The results of our models are then compared to the observations of US 708 to assess its proposed origin from a SN Ia ejection.

The methods, the companion models and the SN Ia explosion model used in this study are described in Section 2. In Section 3 we present the results of 3D simulations of ejecta-donor interaction and 1D post-explosion evolution calculations of the surviving companion stars. A comparison with the observation of US 708 and some discussion of our models is given in Section 4. The main conclusions are summarized in Section 5.

2. Numerical methods and models

We construct the initial He star companion models at the moment of SN Ia explosion based on a SN explosion model within the sub-Chandrasekhar mass DDet scenario of [Gronow et al. \(2020\)](#). We describe in detail the initial conditions and setup for our 3D hydrodynamic impact simulation, the conversion between the 3D Smooth Particle Hydrodynamics (SPH) models and the 1D model, as well as the 1D post-impact evolution of a surviving companion star.

2.1. Code for the ejecta-donor interaction

To obtain the detailed post-explosion properties of surviving companion stars of SNe Ia, we perform a 3D hydrodynamic simulation of SN ejecta-companion interaction with the SPH code STELLAR GADGET ([Springel 2005](#); [Pakmor et al. 2012](#)). The initial conditions and basic setup for the impact simulation of this work are similar to those in our previous impact studies (e.g., [Liu et al. 2012, 2013b,c,a](#)). The companion star at the moment of SN explosion and the SN ejecta model are the two fundamental inputs of our hydrodynamic impact simulation, and we discuss our setups for these two models below.

2.1.1. The He-star donor model

[Geier et al. \(2015\)](#) proposed a double detonation SN explosion resulting from a binary progenitor system composed of a WD with $M_{\text{WD}}^i = 1.05 M_{\odot}$ and a $M_2^i = 0.45 M_{\odot}$ He-burning companion star with an initial orbital period of $P^i \simeq 0.0182$ days as a possible origin of US 708. In their model, the first detonation is assumed to be triggered when the mass of the accreted He shell reaches $M_{\text{He}} = 0.15 M_{\odot}$. The surviving donor He star of $M_2^f = 0.30 M_{\odot}$ is ejected from the system. In this model, the He donor has an orbital velocity of $V_{\text{orb}} \simeq 920 \text{ km s}^{-1}$ at the moment of SN Ia explosion. This can explain the observed high velocity of US 708 (1200 km s^{-1} ; [Geier et al. 2015](#)). [Woosley & Kasen \(2011\)](#); [Bildsten et al. \(2007\)](#); [Shen & Bildsten \(2009\)](#); [Shen & Moore \(2014\)](#); [Shen et al. \(2018\)](#), for example, suggest that a massive WD could trigger a He detonation by accreting a rather thin He shell from its companion star. For this scenario, recent 2D/3D hydrodynamic models of SN Ia explosion have also shown that a core detonation is still possible despite the weaker He shell detonation ([Fink et al. 2010](#); [Sim et al. 2010](#); [Townsend et al. 2019](#); [Gronow et al. 2020, 2021](#)). This seems to indicate that a massive initial WD of $\sim 1.05 M_{\odot}$ is likely to accumulate a thin He shell rather than the $0.15 M_{\odot}$ required otherwise to successfully

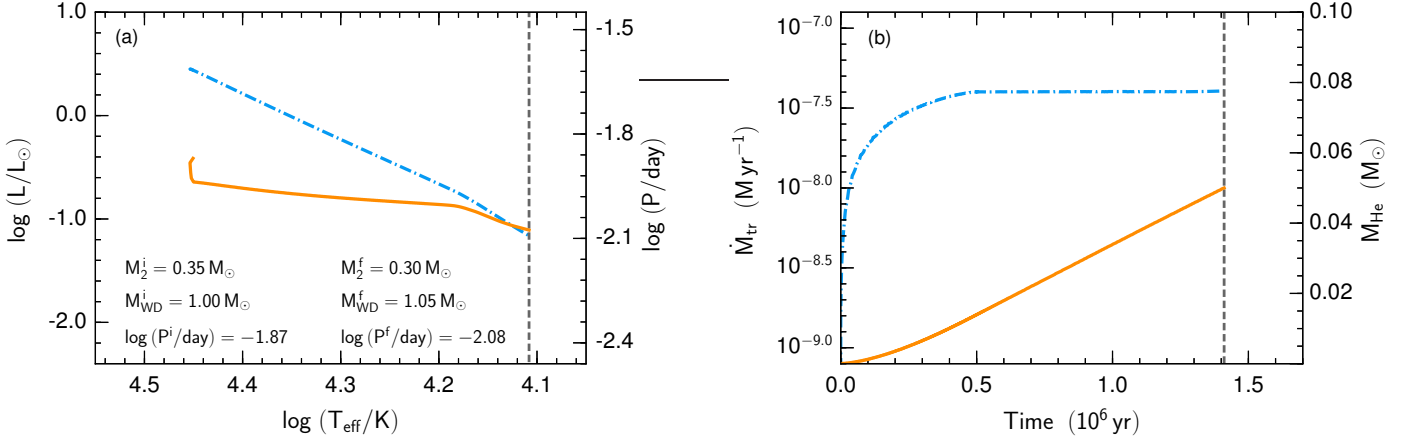


Fig. 1. **Left Panel:** evolutionary tracks of the luminosity of He-star companion (cyan dash-dotted line) and the orbital period of the binary system (orange solid line) during the whole mass-transfer process until the SN Ia explosion. **Right Panel:** time evolution of the mass transfer rate (\dot{M}_{tr} , cyan dash-dotted line) and the mass-growth of a helium shell onto the WD (M_{He} , orange solid line). The vertical dotted lines give the moment of the SN explosion. The initial and final binary parameters (WD mass M_{WD} , companion mass M_2 , orbital period P) in our detailed binary calculations are shown in the plot and indicated with superscript letters ‘i’ and ‘f’, respectively.

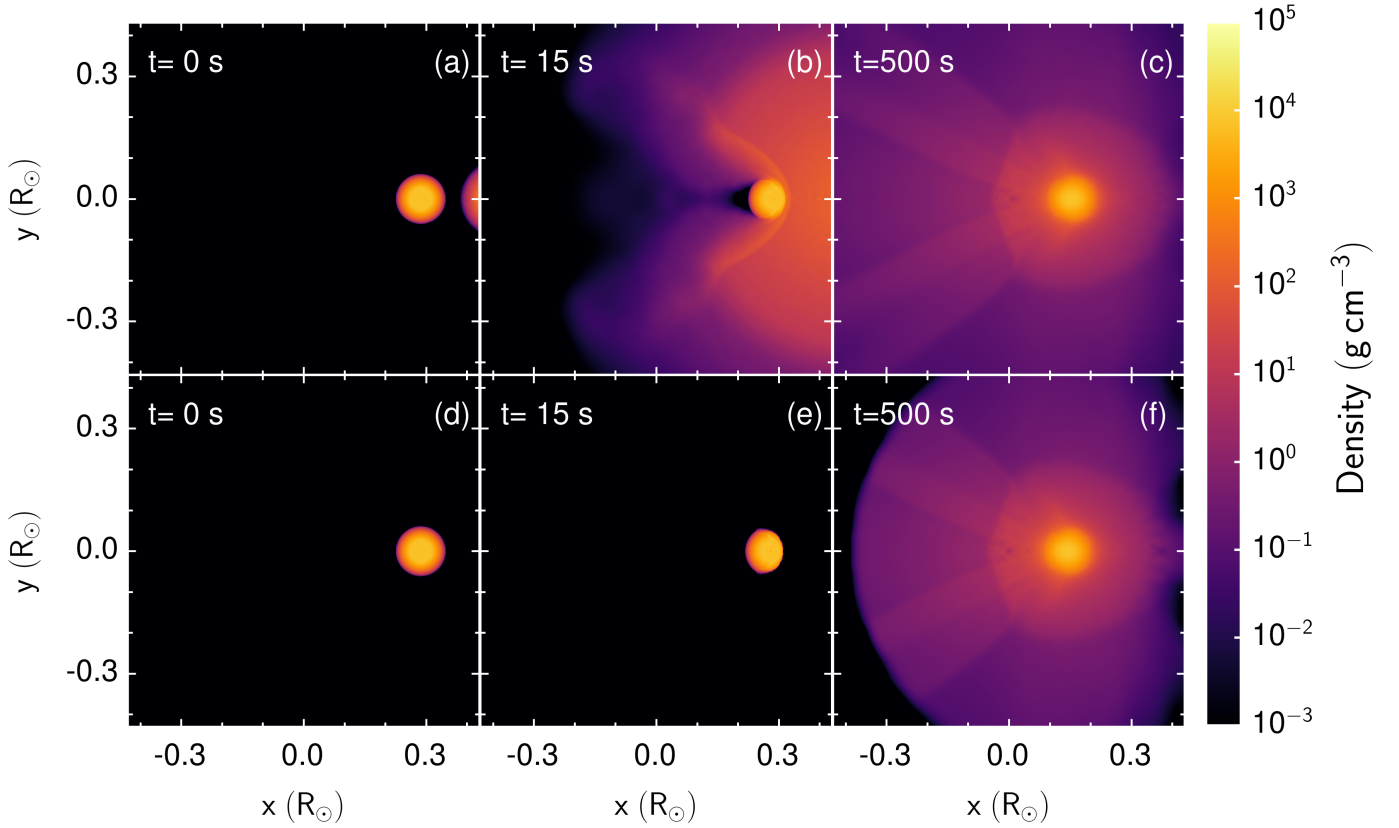


Fig. 2. Density distributions of all material (Panels a–c) and of the bound companion material (Panels d–f). The panels show a slice in the orbital plane in for three different times each. Colours indicate density as per colour bar (right). The 3D hydrodynamical simulation of the SN ejecta-companion interaction shown here does not include binary orbital motion and stellar spin. All panels use the same length scales.

trigger a thermonuclear explosion by undergoing a double detonation.

We adopt the method of Geier et al. (2015) to construct the He-star donor model at the moment of explosion by performing binary evolution calculation using the 1D stellar evolution

code MESA (Paxton et al. 2011, 2015, 2018)¹. As detailed in Sect. 2.1.2, our goal is to directly connect to the DDet Model

¹ Geier et al. (2015) used the Cambridge stellar evolution code STARS (Eggleton 1971, 1972; Pols et al. 1995; Stancliffe 2010) for their binary evolution calculations. When a consistent setup is adopted, we find that the donor structures and binary parameters are identical between the MESA and the STARS models at the moment of SN explosion.

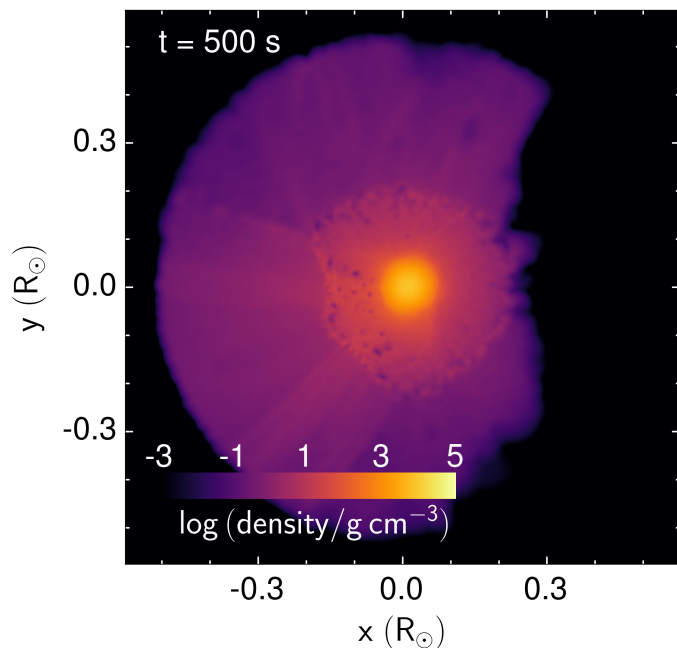


Fig. 3. Similar to Fig. 2f, but for the 3D simulation that includes binary orbital motion and stellar spin.

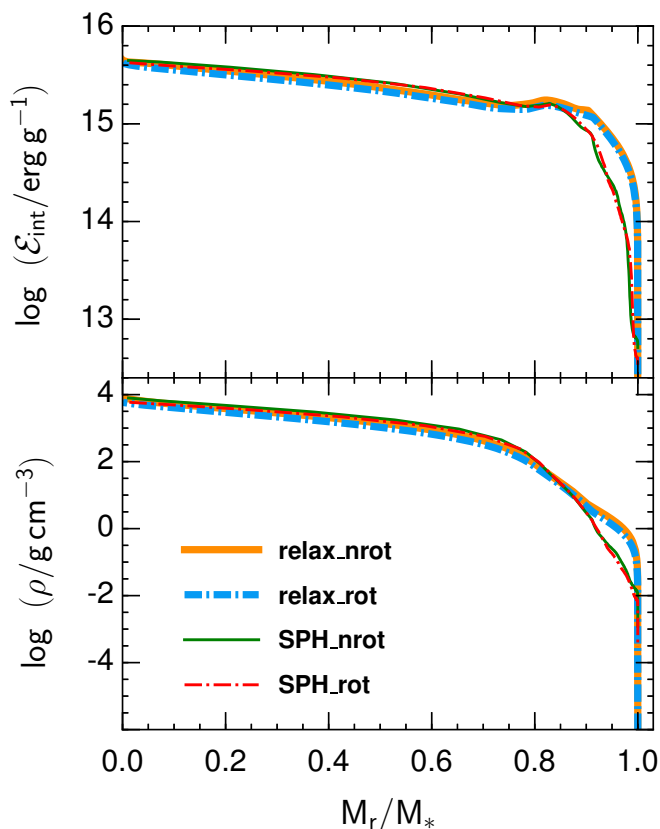


Fig. 4. Post-impact 1D angle-averaged profiles (*thin lines*) of specific internal energy \mathcal{E}_{int} (*Top Panel*) and density ρ (*Bottom Panel*) as functions of fractional mass coordinate at the end of the SPH impact simulation for our reference Model A. For a comparison, the relaxed starting model in MESA are shown as *thick lines*. The results for the impact simulation with (or without) binary orbital motion and stellar spin taken into account are shown as *dash-dotted lines* and *solid lines*, respectively.

M2a² of Gronow et al. (2020). We therefore diverge from the system parameters given by Geier et al. (2015) and start our consistent binary evolution calculation with a progenitor system consisting of an initial WD ($M_{\text{WD}}^i = 1.00 M_{\odot}$) and a He-burning star ($M_2^i = 0.35 M_{\odot}$) with an orbital period of $P^i \simeq 0.0135$ days (Table 1). Figure 1 shows key parameters of the detailed binary evolution calculation of the He-star donor model used for our reference impact simulation. The initial He companion model is set up with a He abundance of $Y = 0.98$, with a metallicity of $Z = 0.02$, and the WD is treated as a point mass in our binary evolution calculation. This binary system starts mass transfer when the He donor star fills its Roche lobe. The orbital angular momentum loss due to gravitational wave radiation is included by following the standard formula given by Landau & Lifshitz (1971). According to previous works, at a mass transfer rate of $\dot{M}_{\text{tr}} < 4.0 \times 10^{-8} M_{\odot} \text{yr}^{-1}$ the He shell builds up steadily, avoiding He burning (e.g., Woosley et al. 1986; Ruiter et al. 2014). Matching to the hydrodynamic explosion model M2a of Gronow et al. (2020, see their Table 1), the double-detonation is assumed to trigger when the He-shell mass reaches a critical value of $M_{\text{He}}=0.05 M_{\odot}$ (see also Fink et al. 2010).

For our binary evolution simulation we obtain a He donor model with a mass of $M_2^i \simeq 0.30 M_{\odot}$ (Fig. 1) at the moment of SN Ia explosion. This model is used as input of our 3D supernova explosion impact simulation. This is our reference model (Table 1). The properties of this companion model, its density profile, the orbital velocity of $V_{\text{orb}} \simeq 901 \text{ km s}^{-1}$, and the effective temperature of $\log_{10} T_{\text{eff}} \simeq 4.1$, are quite similar to those suggested by Geier et al. (2015) for US 708.

2.1.2. The SN explosion model

Our binary progenitor models are constructed to match the hydrodynamic simulation Model M2a of Gronow et al. (2020) for a double-detonation sub-Chandrasekhar mass SN Ia explosion. We directly adopt their Model M2a to represent SN Ia explosion here. This model has masses of the exploding star, of the C/O core, and of the He shell that are $M_{\text{tot}} \approx 1.05 M_{\odot}$, $M_{\text{core}} \approx 1.00 M_{\odot}$, and $M_{\text{shell}} \approx 0.05 M_{\odot}$, respectively (Gronow et al. 2020, see their Table 1). The total explosion energy is about 1.25×10^{51} erg, and the average velocity of the ejecta is of the order 10^4 km s^{-1} . Gronow et al. (2020) and Fink et al. (2010) provide a detailed description of this explosion model. In addition, Gronow et al. (2020) present the results of a time-dependent multi-wavelength radiative transfer calculations for this model.

2.1.3. Initial setup

As described in Pakmor et al. (2012), we use the HEALPix method (Górski et al. 2005) to map the 1D profiles of density and internal energy of our He-star donor model to a particle distribution suitable for the 3D SPH code (see also Liu et al. 2012, 2013b,c,a). Before we start the actual impact simulation, the SPH model of each donor star is relaxed for ten dynamical timescales, $t_{\text{dyn}} = 1/2 (G\rho)^{-1/2}$, to reduce numerical noise introduced by the mapping (e.g., Pakmor et al. 2012; Liu et al. 2012).

For our reference simulation, about 1.8×10^7 SPH particles are used in total to represent both the He companion star and the explosion model. All SPH particles are assigned the same

² Model M2a was constructed to be similar to the Model 3 of Fink et al. (2010), and it was presented as the reference model in Gronow et al. (2020).

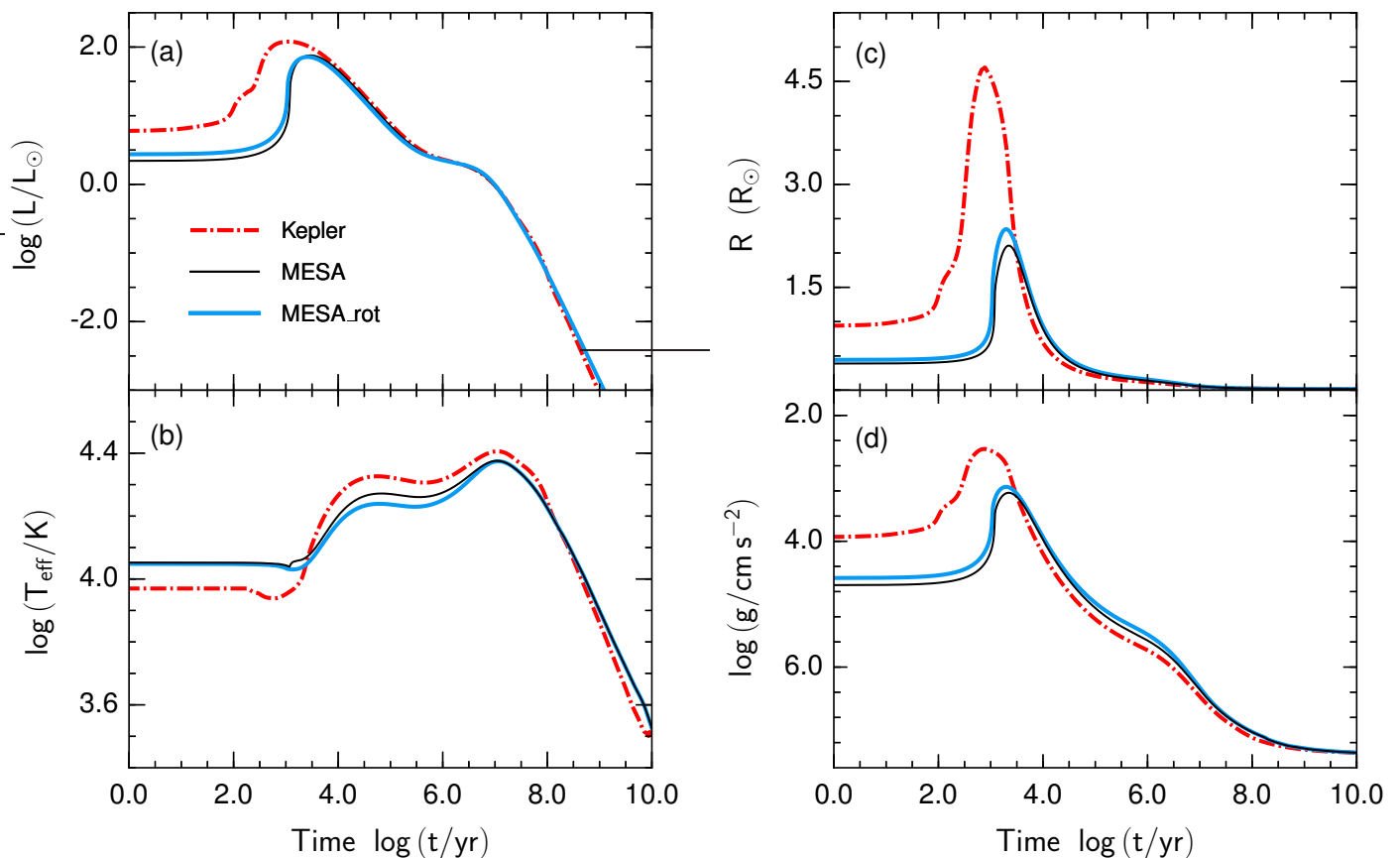


Fig. 5. Post-impact evolution of the photosphere luminosity, L , effective temperature, T_{eff} , radius, R , and surface gravity, g , of a surviving He star companion as functions of time. The *solid line* and *dash-dotted line* respectively correspond to the results from 1D calculations using the KEPLER code and by the MESA code. For comparison, the MESA results based on the impact simulations that do and do not include the binary orbital motion and stellar spin are given as *thick solid line* and *thin solid line*, respectively.

mass of about $7.4 \times 10^{-8} M_{\odot}$. Once the relaxation of the He-star donor is finished, the double-detonation sub-Chandrasekhar explosion model described above is placed at the distance to the donor star that given by the binary separation at the moment of SN Ia initiation in our 1D binary evolution calculation. Based on the 1D-averaged radial profiles of Model M2a of Gronow et al. (2020), SPH particles are placed randomly in shells to reproduce the density profile. The chemical composition and radial velocity of each particle are set to the values of the initial 1D explosion model at a given radius. The ejecta-companion interaction is then simulated for several thousands of seconds until it has ceased and the total stripped mass and kick velocity received by the donor due to the interaction have saturated.

For our second set of impact simulations that take into account the orbital and stellar spin velocities of the companion star, we assume that the companion star co-rotates with its orbit due to strong tidal interaction during pre-explosion mass-transfer phase. This leads to locking of the spin period of the companion star with its orbital period. The companion star is assumed to rotate as a solid body. To isolate the impact of the binary model parameters, we use the same explosion model described in Section 2.1.2 in all simulations presented of this work.

2.2. Mapping from 3D to 1D

Predicting the observable properties of a surviving companion star in the supernova remnant phase requires to model its post-

impact evolution over a few hundred years after the SN Ia explosion. Since the time step in our 3D SPH impact simulations is on the order of the dynamical timescale – hundreds of seconds – this is not possible in the framework of our 3D hydrodynamic simulation. To limit the computational cost of the simulation to a reasonable wall clock time, the outcome of 3D impact simulations is mapped into the 1D stellar evolution code MESA by using the method of Liu & Zeng (2021, see their Section 2) to trace the subsequent long-term post-explosion evolution (see also Pan et al. 2013, 2014; Bauer et al. 2019). The three main steps of this method are briefly summarized in the following: First, the 3D post-impact companion models from our hydrodynamic impact simulations (Fig. 2f) are converted into 100–200 spherical shells. The physical properties of the SPH particles, such as the internal energy and composition, are averaged to give a value for that shell. Second, the 1D averaged radial profiles of internal energy, chemical composition, and density are used as inputs for the MESA code to compute suitable starting models for the subsequent post-explosion calculations by directly adopting the relaxation routines provided in MESA (Paxton et al. 2018, see their Appendix B). Third, we follow long-term evolution of a surviving companion model to predict its observable properties until it enters the WD cooling phase.

We use the MESA code in its hydrostatic mode and therefore artificially relax our hydrodynamic post-impact model to hydrostatic equilibrium. To test the effect of this approximation, we additionally perform a simulation of the post-impact evolu-

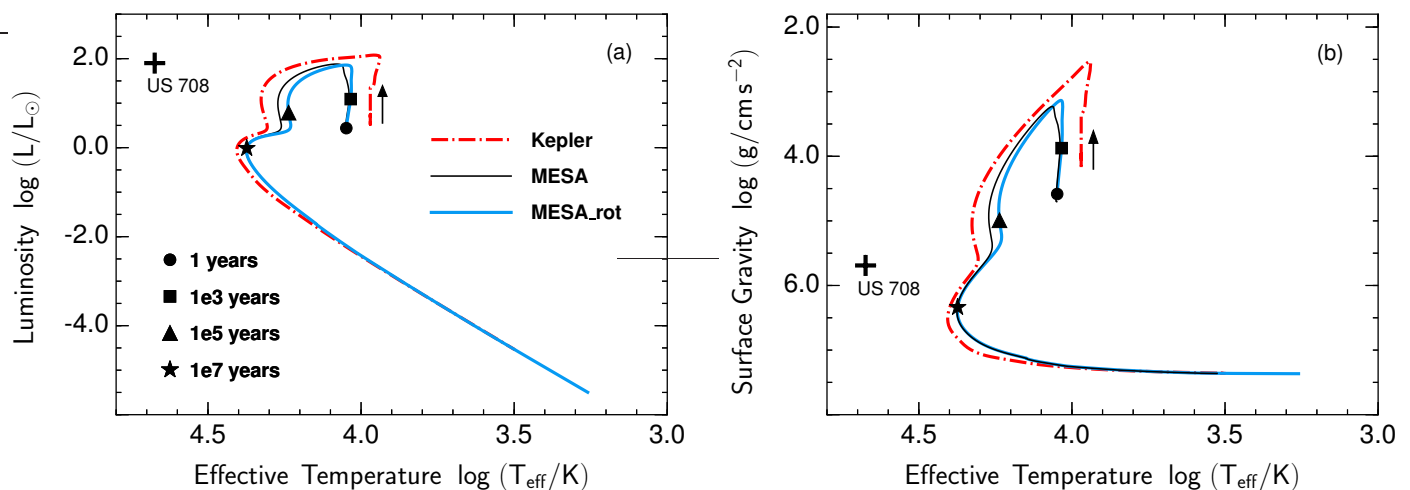


Fig. 6. Post-impact evolutionary tracks of a surviving He star companion model in the Hertzsprung-Russell Diagram (*Left Panel*) and surface gravity vs. temperature diagram (*Right Panel*). The *solid lines* and *dash-dotted lines* respectively correspond to the results of *KEPLER* and *MESA* calculations. The *filled circle*, *square*, *triangle*, and *star* markers on the tracks present post-impact evolutionary phases of 1 yr, 1 kyr, 100 kyr, and 10 Myr after the SN impact, respectively. The *thin lines* and *thick lines* have the same meaning as those in Fig. 5.

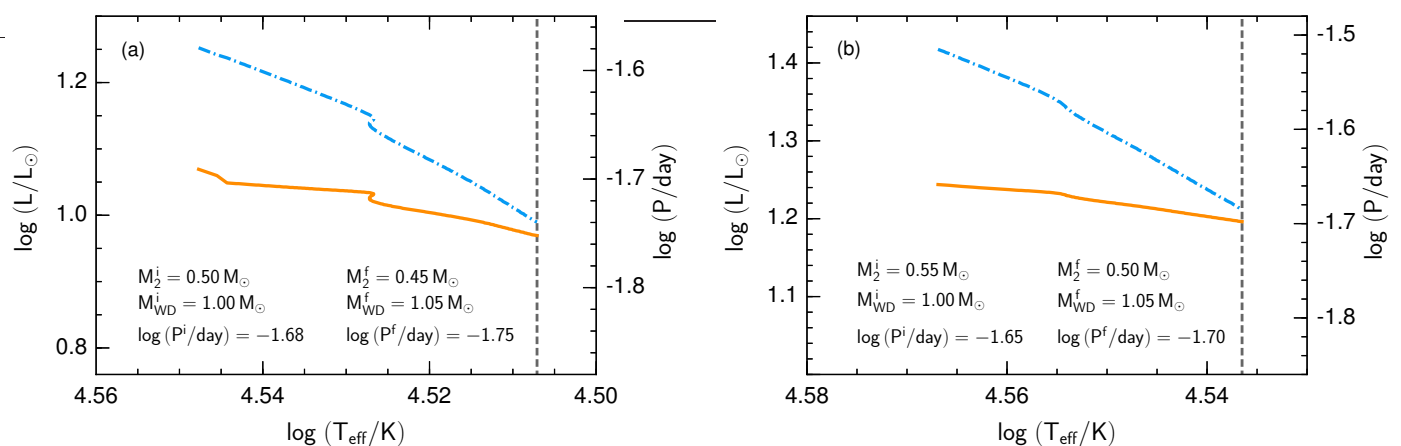


Fig. 7. Similar to the *Left Panel* of Fig. 1, but for two more massive He-star donor models with initial masses of $0.50 M_{\odot}$ (*Left Panel*) and $0.55 M_{\odot}$ (*Right Panel*).

tion for our reference model with the 1D hydrodynamic stellar evolution code *KEPLER* (Weaver et al. 1978; Rauscher et al. 2002; Woosley et al. 2002; Heger & Woosley 2010). Similarly, the angle-averaged 1D radial profiles obtained from 3D post-impact companion models are used as inputs of the subsequent *KEPLER* calculations, but without performing any relaxation process. In addition, we include the radial velocity of each spherical shell at the end of our impact simulation into the *KEPLER* models. This way the hydrodynamics is also followed from the beginning of the mapping in the *KEPLER* calculations. We find no significant difference between *MESA* and *KEPLER* results for our reference calculation for Model A (Section 3.2). For consistent analysis and discussion, all other He-star donor models in Section 4.2 are only simulated using the *MESA* code.

3. Numerical results

In this section, we present the results of 3D hydrodynamic simulations of ejecta-companion interaction. The 1D post-explosion evolution calculations of the surviving companion stars with the *MESA* and *KEPLER* code are also given.

3.1. Ejecta-donor interaction

Figure 2 shows the density distribution of all material (top row) and bound donor material (bottom row) as a function of time in our 3D impact simulation for our reference He-star donor model (Model A). The figure is oriented such that the SN explodes at right-hand side of the donor star. After the explosion, the SN ejecta expand freely for a while (a few 10 seconds) and hits the surface of donor star, stripping some He-rich material from its surface and forming a bow shock. Subsequently, the bow shock propagates through the donor star (Fig. 2b), removing more He-rich material from the far side of it. The donor star is significantly shocked and heated during the interaction with the supernova blast wave. It inflates dramatically, but survives the interaction and starts to relax (Fig. 2f). The stripped He-rich donor material is largely embedded in the low-velocity SN debris behind the star. Quantitative details of the models and of the simulation results are summarised in Table 1.

At the end of our 3D simulation, we find that the total amount of stripped He material from the donor surface during the ejecta-donor interaction is about $\Delta M \approx 0.02 M_{\odot}$, i.e., about 6% of

Table 1. Three He donor models studied by this work.

Model	M_{WD}^i	M_2^i	M_2^f	$\log P^f$	$\log T_{\text{eff}}^f$	a^f	R_2^f	V_{orb}^f	V_{rot}^f	$\Delta M/M_2^f$	V_{kick}	L_{peak}	t_{peak}	E_{in}
	(M_{\odot})	(M_{\odot})	(M_{\odot})	(days)	(K)	(10^{10} cm)	(km s^{-1})	(km s^{-1})	(%)	(km s^{-1})	($10^3 L_{\odot}$)	(10^3 yr)	(10^{49} erg)	
A	1.00	0.35	0.30	-2.08	4.10	1.34	0.37	901	320	5.7	201	0.08	2.96	1.15
B	1.00	0.50	0.45	-1.75	4.50	2.28	0.70	654	288	3.1	95	1.48	0.06	1.07
C	1.00	0.55	0.50	-1.70	4.53	2.50	0.77	614	287	2.8	83	2.09	0.04	1.08

Notes. M_{WD}^i and M_2^i are the initial masses of the WD and donor at the beginning of mass transfer. M_2^f , P^f , T_{eff}^f , a^f , R_2^f , V_{orb}^f , and V_{rot}^f denote the final mass, orbital period, the effective temperature, the binary separation, the radius, the orbital velocity, and the rotational velocity of donor star at the moment of SN explosion, respectively. We assume that the He donor star is tidally locked to its orbital motion. ΔM and V_{kick} are the total stripped donor masses and kick velocity caused by SN impact. L_{peak} and t_{peak} give the peak luminosity and the corresponding post-impact evolutionary time of our MESA models before the deposited energy is radiated away, i.e., before the stars go back to the thermal equilibrium state. E_{in} corresponds to the total amount of energy deposited into the donor star due to the interaction with SN Ia ejecta.

the total donor mass. The donor star receives a kick velocity of $v_{\text{kick}} \approx 200 \text{ km s}^{-1}$, which moves its remnant to left by about 10^{10} cm at 500 s after the explosion (Fig. 2f). The impact simulations for our reference donor model are ran with or without including binary orbital motion and stellar spin to test their effect on the results. Since the orbital and spin velocities of the donor star are much lower than the typical expansion velocity of SN ejecta of our explosion model ($\sim 10^4 \text{ km s}^{-1}$ according to Gronow et al. 2020), only small differences (less than 5%) in the total amount of stripped donor mass and in the kick velocity are observed when the binary orbital motion and stellar spin are included. This is consistent with previous works (e.g., Liu et al. 2013b,c; Pan et al. 2012c). The density distribution of the ejected donor remnant from our impact simulations that includes binary orbital motion and stellar spin is shown in Fig. 3. More asymmetric features in the morphology are observed for this case compared with that shown in Fig. 2f.

3.2. 1D post-impact evolution

As described in Section 2.2 (see also Liu & Zeng 2021), the final outcomes of our 3D impact simulations (Fig. 3) are used to construct the initial inputs for the MESA and KEPLER codes to model the long-term post-impact evolution of the surviving donor stars. Figure 4 shows a comparison between 1D-averaged internal energy and density profiles of our reference model (i.e., Model A in Table 1) at the end of impact simulation and of the corresponding post-relaxed profiles in MESA.

Figure 5 shows the post-impact evolution of photospheric luminosity, L , the effective temperature, T_{eff} , the radius, R , and the surface gravity, g , as functions of time for our reference model (Model A in Table 1). The donor star is significantly shocked by the SN impact during the ejecta-donor interaction. This leads to an energy deposition of 1.15×10^{49} erg. This value has been calculated by tracing the increase in binding energy of the star after the SN Ia impact (see also Pan et al. 2012a; Liu & Zeng 2021). We find that $\sim 50\%$ of the incident energy of the SN Ia ejecta, about 2.30×10^{49} erg³, is injected into the donor star during the ejecta-donor interaction. The donor star continues to expand dramatically for about 1,000 years before it starts to contract (Fig. 5). This expansion timescale is determined by the local radiative diffusion timescale of the donor envelope at the shell where it contains the injected energy from the SN Ia ejecta (Henyey & L'Ecuyer 1969, see their Eq. 49). This expansion

³ Here, the incident energy of SN ejecta is obtained for a ratio of binary separation to companion radius at the moment of SN explosion of $a^f/R_2^f = 3.61$ (see Table 1).

makes the post-impact donor star much more luminous ($\gtrsim 80 L_{\odot}$; Fig. 5) than its pre-explosion brightness. A few thousand years after the explosion, the radius and luminosity of the ejected donor star decreases again as it starts to contract, releasing gravitational energy while the deposited energy radiates away (Fig. 5; Kelvin Helmholtz contraction). Figure 6 shows the post-impact evolution tracks of the ejected donor in the Hertzsprung-Russell (H-R) diagram and in the effective temperature-surface gravity ($T_{\text{eff}} - g$) diagram.

We find that including the binary orbital motion and stellar spin in 3D impact simulations have no significant effect on the post-impact evolution of the surviving donor stars (Figs. 5 and 6). For a comparison, the post-impact evolution of the ejected donor has also been calculated with the KEPLER code. As shown in Figs. 5 and 6, the KEPLER model has a larger radius thus being more luminous than the MESA model. The difference between the KEPLER and the MESA results is attributed to the circumstance that the output models at the end of 3D impact simulations is still somewhat out of equilibrium. Nonetheless, the evolution trends in two approaches are very similar, and no significant difference is observed between these two models (Figs. 5 and 6). This indicates that at the time of the mapping from 3D to 1D the SPH models are already very close to hydrostatic equilibrium (Fig. 4).

4. Discussion

4.1. Comparison with US 708

At the time when the SN explodes in our binary evolution calculation of Model A the donor star has an orbital velocity of $V_{\text{orb}} = 901 \text{ km s}^{-1}$ and a surface rotational velocity of $V_{\text{rot}} = 320 \text{ km s}^{-1}$ (Table 1). We directly obtain from our impact simulation that this star receives a kick velocity of about $V_{\text{kick}} \approx 210 \text{ km s}^{-1}$ due to the ejecta impact (Section 3.1). This kick velocity was simply assumed to be 200 km s^{-1} by (Geier et al. 2015). Therefore, we expect the donor remnant to be ejected with a velocity of $V_{\text{spatial}} = (V_{\text{orb}}^2 + V_{\text{kick}}^2)^{1/2} \approx 925 \text{ km s}^{-1}$. This velocity is dominated by the donor's pre-explosion orbital velocity. This spatial velocity provides a good explanation to the observed high velocity of US 708 of $\sim 1,200 \text{ km s}^{-1}$ (Table 1 of Geier et al. 2015).

Based on the effective temperature of $T_{\text{eff}} = 47,200 \pm 400 \text{ K}$, and the surface gravity of $\log_{10}(g/\text{cm s}^{-2}) = 5.69 \pm 0.09$, given by Geier et al. (2015), the luminosity of US 708 can be simply calculated using $L = 4\pi R^2 \sigma_{\text{SB}} T_{\text{eff}}^4$ under the assumption that the mass of US 708 is $M = 0.3 M_{\odot}$ (see also Bauer et al. 2019). The constant σ_{SB} is the Stefan-Boltzmann constant, as usual. Figure 6 shows a comparison between the properties of the ejected

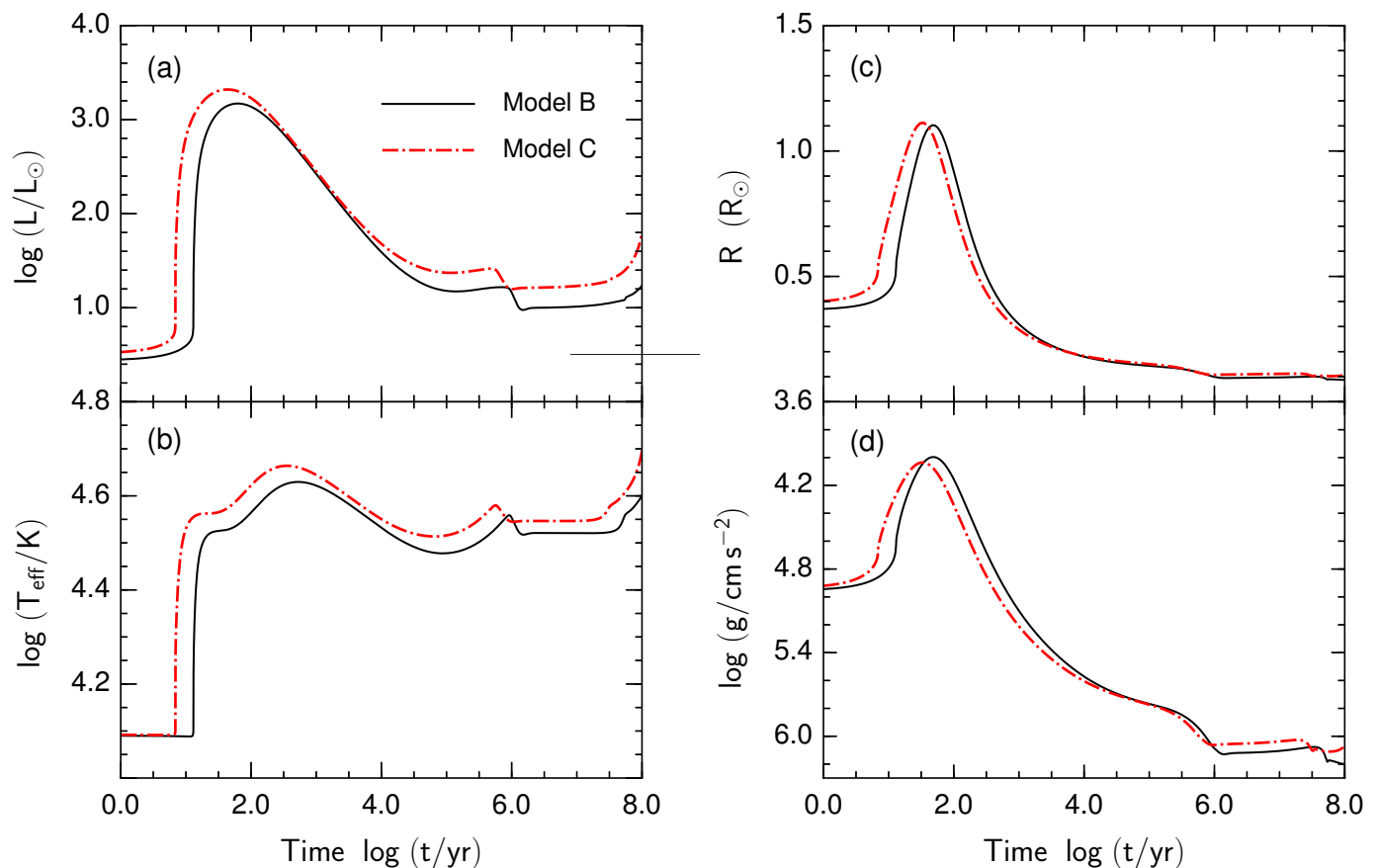


Fig. 8. Similar to Fig. 5, but for the more massive He-star donor models with a post-impact mass of $0.45 M_{\odot}$ (i.e., Model B, see solid black line) and $0.50 M_{\odot}$ (i.e., Model C, see red dash-dotted line).

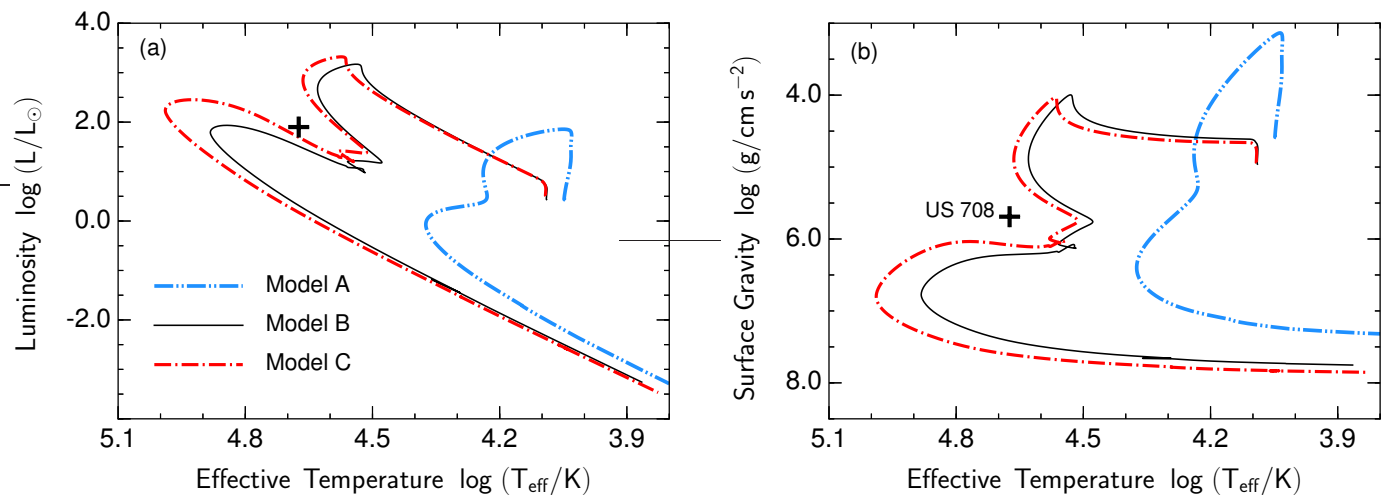


Fig. 9. Similar to Fig. 6, but for the more massive He-star donor models with a post-impact mass of $0.45 M_{\odot}$ (solid black line) and $0.50 M_{\odot}$ (red dash-dotted line). For a comparison, the results of $0.30 M_{\odot}$ He donor model of Fig. 6 is shown as a double-dotted line. The observed properties of US 708 are indicated as a black plus '+'. '.

He donor remnant, its luminosity, effective temperature, and surface gravity, as predicted by our simulations, and those observed for US 708. During its entire post-impact evolution, our Model A stays too cool to pass through the positions of US 708 in the H-R diagram and in the $T_{\text{eff}} - g$ diagram. This suggests that a low-mass donor remnant ($\lesssim 0.3 M_{\odot}$) from a DDet SN Ia cannot easily reproduce the observational properties of US 708. In the

next section we explore whether a more massive ejected donor remnant from a DDet SN Ia could match the observations of US 708, including its luminosity and effective temperature.

Geier et al. (2015) use the long-term evolution of a He-star without any ejecta-donor interaction to fit the observational properties of US 708. As shown in Figs. 5 and 6, the SN impact and heating during the ejecta-donor interaction play an impor-

tant role in the post-impact evolution of a surviving companion star from a DDet SN Ia before it reestablishes thermal equilibrium over the Kelvin-Helmholtz timescale. All energy deposited into the donor star by the SN blast wave has radiated away about 10^6 yr after the explosion. The star relaxes back into thermal equilibrium and continues to evolve by following an evolutionary track very close to that of a He-star with the same mass that has not been impacted and heated by the ejecta-donor interaction. As mentioned above, based on its kinematics US 708 was ejected from the Galactic disc about 14 Myr ago (Geier et al. 2015). At these late epochs after the explosion, the thermal effects of ejecta-donor interaction on the evolution of the surviving He-star becomes negligible. This suggests that the ejecta-donor interaction does not play an important role in explaining the current observational properties of US 708 if it is indeed an ejected donor remnant from a DDet SN Ia.

4.2. More massive donor models

By neglecting the effect of ejecta-donor interaction, Geier et al. (2015) have suggested that the evolutionary track of a post Extended Horizontal Branch (EHB) star with an original mass of $0.45 M_{\odot}$ passes the position of US 708 in the effective temperature-surface gravity diagram. Following their suggestion, we also generate two He-star donor models with a larger initial masses to check whether the post-impact properties of a more massive ejected donor remnant in a DDet SN Ia would match the observations of US 708 better. Model B has an initial mass of $0.50 M_{\odot}$ and Model C has an initial mass of $0.55 M_{\odot}$ (Table 1). For both model we follow the method described in Section 2.1.1. The detailed binary evolution calculations are shown in Fig. 7. In Model B the donor star has a mass of $0.45 M_{\odot}$ at the moment of SN explosion, and Model C reaches a mass of $0.50 M_{\odot}$ at SN explosion of the accreting WD. The key properties of both models are summarised in Table 1. With these models we repeat the 3D modelling of ejecta-donor interaction and 1D post-impact evolution calculations in the same fashion as for Model A and compare to the observational properties of US 708.

Figures 8 and 9 show the detailed post-impact properties and evolution tracks of Models B and C. These more massive surviving He-star donors reach their peak luminosities of $(1.5-2.1) \times 10^3 L_{\odot}$ at $\lesssim 60$ yr, much faster than the $\sim 3,000$ yr needed in Model A. The energy deposition in the more massive models occurs at lower depths, leading to a shorter local radiative diffusion timescale of the donor envelope. Additionally, the total amounts of energy deposition from SN ejecta in these two models are smaller than that in Model A (Table 1). A fundamental and qualitative difference is that donor models with $> 0.3 M_{\odot}$ show He burning as they contract. As the deposited energy is radiated away, their temperature increases significantly (about 10^7 yr after the explosion) with an almost fixed radius and luminosity before they enter the WD cooling stage (Figs. 8 and 9). Our most massive ejected donor remnant model ($\sim 0.5 M_{\odot}$) becomes bright and hot enough to achieve the observed luminosity and temperature of US 708 (Geier et al. 2015). Unfortunately, with $\log_{10}(g/\text{cm s}^{-2}) \approx 6.20$, it has a higher surface gravity than that of US 708. This could indicate that an even more massive He-star donor model may be needed to match the observations of US 708. However, our detailed binary evolution calculations indicates that a binary progenitor system with such a massive He-star donor is unlikely to be close enough to reach a sufficiently high orbital velocity at the moment of SN explosion (Table 1), and hence would fail to explain the observed high spatial velocity of US 708.

Our results and conclusions are similar to those presented by Geier et al. (2015). Figs 8 and 9 show that our surviving companion stars have re-established thermal equilibrium completely about 14 Myr after the explosion. At these late epochs, the observational properties of our surviving companion stars are not sensitive to the details of ejecta-donor interaction, and are thus similar to those of EHB-star models with the same mass adopted by Geier et al. (2015) at similar epochs. This confirms that neglecting the effect of ejecta-donor interaction for the comparison with US 708 is a reasonable approximation.

Low-mass donors not becoming bright enough and high-mass donors not becoming fast enough pose problems for explaining US 708 as the He-star donor ejected from a DDet SNe Ia. An alternative explanation would be that the pre-explosion binary progenitor system has travelled at a speed of about 400 km s^{-1} into the direction of its current motion (see also Brown et al. 2015; Bauer et al. 2019).

4.3. Uncertainties and future work

In this work, the He-star donor models are constructed based on a sub-Chandrasekhar mass double-detonation explosion model given by Gronow et al. (2020). The exact critical He shell mass required to successfully initiate a the thermonuclear SN explosion by triggering double detonations is still quite uncertain (e.g., Woosley & Kasen 2011; Bildsten et al. 2007; Shen & Moore 2014; Townsley et al. 2019; Gronow et al. 2021). Our investigation is inherently limited by the assumption of a critical He-shell mass of $\sim 0.05 M_{\odot}$. Different core and He shell masses of exploding WDs could significantly affect the SN ejecta properties and thus the predicted observational features of the resulting SNe Ia (e.g., Gronow et al. 2021). This introduces some uncertainties into the firmness of our conclusions. Nevertheless, we do demonstrate that certain companion masses are promising for reproducing US 708, and therefore we think that such a model seems likely to explain the main features of this star.

The exact He-retention efficiency of the accreting WD in the progenitor system is still poorly constrained (e.g., Ruiter et al. 2014; Toonen et al. 2014). This is expected to add to the uncertainties of our 1D binary evolution calculation providing the binary properties and donor structures at the time of SN explosion. To comprehensively model the predictions on the observables of surviving donors of DDet SNe Ia and to improve the fit with US 708, more donor models need to be constructed and investigated. Our future work will include different DDet explosion models covering a range of core and He shell masses of exploding WDs.

In our impact simulations, we find that some SN ejecta material are captured by the donor star during the ejecta-donor interaction. The decay of the deposited radioactive elements (e.g., ^{56}Ni) could re-heat the donor star and thus affect its post-impact evolution (e.g., Shen & Schwab 2017). We leave a detailed study of the influence of captured ejecta elements on the post-impact evolution of a surviving companion star of a DDet SN Ia to a future work.

5. Summary

For the first time, we have consistently performed 3D hydrodynamical simulations of ejecta-donor interaction within the DDet scenario of SNe Ia. We then follow the long-term post-impact evolution of surviving He-star companions of DDet SNe Ia by combining the outcomes of 3D hydrodynamic impact simulations into 1D post-impact evolution codes. We have provided the

observable signatures of the surviving companion stars of DDet SNe Ia, which can guide the search for such companion stars with future observations. We also compare our results to the observations of the hypervelocity star US 708 to assess the validity of explaining the origin of this star with an ejected He donor from a DDet SNe Ia. The results and conclusions of this work are summarized as follows.

- (1) We find that about 3%–6% of the initial donor mass is stripped off from their outer layers during the ejecta-donor interaction for our three He-star donor models. The donor stars receive impact kick velocities of 80–200 km s⁻¹, resulting in ejected donor remnants spatial velocities of 619–923 km s⁻¹. These velocities are dominated by the pre-explosion orbital velocities of 614–901 km s⁻¹ (Table 1).
- (2) We find that the donors are significantly shocked and heated during the ejecta-donor interaction. In addition, we find that an energy of about $(1.07\text{--}1.15) \times 10^{49}$ erg is deposited into the donor stars, which corresponds to about 35%–48% of the total incident energy from SN ejecta being absorbed by the donor remnants (Table 1). The surviving donor stars inflate for about 100–1,000 yr and reach peak luminosities of $(0.08\text{--}2.2) \times 10^3 L_{\odot}$, exceeding their pre-explosion luminosities by a up to factor of about 800 (Figs. 5 and 8).
- (3) We find that the ejecta-donor interaction plays an important role in determining the post-impact observable signatures of surviving companion stars of DDet SNe Ia during the thermal re-equilibration phase. This leads to that the surviving companion stars become significantly overluminous for the Kelvin-Helmholtz timescale of about 10⁶ yr. After the stars reestablish thermal equilibrium, they continue to evolve by following an evolutionary track very close to that of a He-star with the same mass that has not been impacted and heated due to the ejecta-donor interaction.
- (4) Although our reference model (Model A) matches the high velocity of US 708 (about 1,200 km s⁻¹, Geier et al. 2015), it does not reproduce the observed temperature and luminosity of this star.
- (5) The US 708 was ejected about 14 Myr ago based on its kinematics (Geier et al. 2015). At these late epochs after the explosion, the observational properties of our surviving companions are not sensitive to the details of the ejecta-donor interaction. Therefore, the ejecta-donor interaction may not play an important role in examining the SN Ia origin of US 708.
- (6) Based on the results (Fig. 9) of our more massive donor star models (Model B and C), we suggest that a He-star donor with an initial mass of $\geq 0.5 M_{\odot}$ is needed to reproduce the observed properties of US 708 such as its luminosity, effective temperature and surface gravity (see also Geier et al. 2015). However, our detailed binary evolution calculations show that such massive donors might not reach sufficiently high orbital velocities at the moment of SN explosion in the DDet scenario to explain the observed high spatial velocity of US 708.
- (7) Explaining the high spatial velocity of US 708 with a massive ejected donor remnant ($\geq 0.5 M_{\odot}$) from a DDet SN Ia event may require that its binary progenitor system has already traveled at a speed of about 400 km s⁻¹ in the observed direction in the galactic halo before the SN explosion (see also Brown et al. 2015).

To determine whether or not US 708 is indeed an ejected donor remnant from a DDet SN Ia requires further improvements

of the binary evolution calculations, in particular of the accumulation efficiency of accreted He material onto the WD, and of the hydrodynamic impact modelling with different DDet explosion models covering a range of core and He shell masses of exploding white dwarfs.

Acknowledgements. We thank the anonymous referee for constructive comments that helped to improve this paper. ZWL would like to thank Robert G. Izzard for his fruitful discussions. ZWL is supported by the National Natural Science Foundation of China (NSFC, No. 11873016), the Chinese Academy of Sciences (CAS) and the Natural Science Foundation of Yunnan Province (No. 202001AW070007). The work of FR is supported by the Klaus Tschira Foundation and by the Deutsche Forschungsgemeinschaft (DFG, German Research Foundation) – Project-ID 138713538 – SFB 881 (“The Milky Way System”, Subproject A10). AH acknowledges support by the Australian Research Council (ARC) Centre of Excellence (CoE) for Gravitational Wave Discovery (OzGrave) project number CE170100004, by the ARC CoE for All Sky Astrophysics in 3 Dimensions (ASTRO 3D) project number CE170100013, and by the US National Science Foundation under Grant No. PHY-1430152 (JINA Center for the Evolution of the Elements). The authors gratefully acknowledge the ‘PHOENIX Supercomputing Platform’ jointly operated by the Binary Population Synthesis Group and the Stellar Astrophysics Group at Yunnan Observatories, CAS. This work made use of the Heidelberg Supernova Model Archive (HESMA, see <https://hesma.h-its.org>, Kromer et al. 2017).

References

- Aarseth, S. J. 1974, *A&A*, 35, 237
- Bauer, E. B., White, C. J., & Bildsten, L. 2019, *ApJ*, 887, 68
- Bildsten, L., Shen, K. J., Weinberg, N. N., & Nelemans, G. 2007, *ApJ*, 662, L95
- Blaauw, A. 1961, *Bull. Astron. Inst. Netherlands*, 15, 265
- Boos, S. J., Townsley, D. M., Shen, K. J., Caldwell, S., & Miles, B. J. 2021, arXiv e-prints, arXiv:2101.12330
- Brown, W. R. 2015, *ARA&A*, 53, 15
- Brown, W. R., Anderson, J., Gnedin, O. Y., et al. 2015, *ApJ*, 804, 49
- Brown, W. R., Geller, M. J., Kenyon, S. J., & Kurtz, M. J. 2005, *ApJ*, 622, L33
- Eggleton, P. P. 1971, *MNRAS*, 151, 351
- Eggleton, P. P. 1972, *MNRAS*, 156, 361
- Fink, M., Hillebrandt, W., & Röpke, F. K. 2007, *A&A*, 476, 1133
- Fink, M., Röpke, F. K., Hillebrandt, W., et al. 2010, *A&A*, 514, A53
- Fryxell, B. A. & Arnett, W. D. 1981, *ApJ*, 243, 994
- Geier, S., Fürst, F., Ziegerer, E., et al. 2015, *Science*, 347, 1126
- Geier, S., Marsh, T. R., Wang, B., et al. 2013, *A&A*, 554, A54
- Geier, S., Nesslinger, S., Heber, U., et al. 2007, *A&A*, 464, 299
- Górski, K. M., Hivon, E., Banday, A. J., et al. 2005, *ApJ*, 622, 759
- Gronow, S., Collins, C., Ohlmann, S. T., et al. 2020, *A&A*, 635, A169
- Gronow, S., Collins, C. E., Sim, S. A., & Roepke, F. K. 2021, arXiv e-prints, arXiv:2102.06719
- Gvaramadze, V. V., Gualandris, A., & Portegies Zwart, S. 2009, *MNRAS*, 396, 570
- Heger, A. & Woosley, S. E. 2010, *ApJ*, 724, 341
- Henyey, L. & L’Ecuyer, J. 1969, *ApJ*, 156, 549
- Hillebrandt, W., Kromer, M., Röpke, F. K., & Ruiter, A. J. 2013, *Frontiers of Physics*, 8, 116
- Hills, J. G. 1988, *Nature*, 331, 687
- Kasen, D. 2010, *ApJ*, 708, 1025
- Kato, M. & Hachisu, I. 2003, *ApJ*, 598, L107
- Kromer, M., Ohlmann, S., & Röpke, F. K. 2017, *Mem. Soc. Astron. Italiana*, 88, 312
- Kudritzki, R. P. & Simon, K. P. 1978, *A&A*, 70, 653
- Landau, L. D. & Lifshitz, E. M. 1971, *The classical theory of fields*
- Leonard, D. C. 2007, *ApJ*, 670, 1275
- Leonard, P. J. T. 1991, *AJ*, 101, 562
- Li, W., Bloom, J. S., Podsiadlowski, P., et al. 2011, *Nature*, 480, 348
- Liu, Z.-W., Kromer, M., Fink, M., et al. 2013a, *ApJ*, 778, 121
- Liu, Z.-W., Pakmor, R., Röpke, F. K., et al. 2013b, *A&A*, 554, A109
- Liu, Z. W., Pakmor, R., Röpke, F. K., et al. 2012, *A&A*, 548, A2
- Liu, Z.-W., Pakmor, R., Seitzzahl, I. R., et al. 2013c, *ApJ*, 774, 37
- Liu, Z.-W. & Zeng, Y. 2021, *MNRAS*, 500, 301
- Livne, E. & Arnett, D. 1995, *ApJ*, 452, 62
- Livne, E., Tuchman, Y., & Wheeler, J. C. 1992, *ApJ*, 399, 665
- Maoz, D., Mannucci, F., & Nelemans, G. 2014, *ARA&A*, 52, 107
- Marietta, E., Burrows, A., & Fryxell, B. 2000, *ApJS*, 128, 615
- Marted, P. F. L., Marsh, T. R., & North, R. C. 2000, *MNRAS*, 317, L41
- Moll, R. & Woosley, S. E. 2013, *ApJ*, 774, 137
- Neunteufel, P. 2020, *A&A*, 641, A52
- Neunteufel, P., Kruckow, M., Geier, S., & Hammers, A. S. 2021, *A&A*, 646, L8

- Neunteufel, P., Yoon, S. C., & Langer, N. 2016, *A&A*, 589, A43
- Pakmor, R., Edelmann, P., Röpke, F. K., & Hillebrandt, W. 2012, *MNRAS*, 424, 2222
- Pakmor, R., Röpke, F. K., Weiss, A., & Hillebrandt, W. 2008, *A&A*, 489, 943
- Pan, K.-C., Ricker, P. M., & Taam, R. E. 2012a, *ApJ*, 760, 21
- Pan, K.-C., Ricker, P. M., & Taam, R. E. 2012b, *ApJ*, 750, 151
- Pan, K.-C., Ricker, P. M., & Taam, R. E. 2012c, *ApJ*, 750, 151
- Pan, K.-C., Ricker, P. M., & Taam, R. E. 2013, *ApJ*, 773, 49
- Pan, K.-C., Ricker, P. M., & Taam, R. E. 2014, *ApJ*, 792, 71
- Paxton, B., Bildsten, L., Dotter, A., et al. 2011, *ApJS*, 192, 3
- Paxton, B., Marchant, P., Schwab, J., et al. 2015, *ApJS*, 220, 15
- Paxton, B., Schwab, J., Bauer, E. B., et al. 2018, *ApJS*, 234, 34
- Perlmutter, S., Aldering, G., Goldhaber, G., et al. 1999, *ApJ*, 517, 565
- Polin, A., Nugent, P., & Kasen, D. 2019, *ApJ*, 873, 84
- Pols, O. R., Tout, C. A., Eggleton, P. P., & Han, Z. 1995, *MNRAS*, 274, 964
- Rauscher, T., Heger, A., Hoffman, R. D., & Woosley, S. E. 2002, *ApJ*, 576, 323
- Riess, A. G., Filippenko, A. V., Challis, P., et al. 1998, *AJ*, 116, 1009
- Ruiter, A. J., Belczynski, K., Sim, S. A., et al. 2011, *MNRAS*, 417, 408
- Ruiter, A. J., Belczynski, K., Sim, S. A., Seitenzahl, I. R., & Kwiatkowski, D. 2014, *MNRAS*, 440, L101
- Schmidt, B. P., Suntzeff, N. B., Phillips, M. M., et al. 1998, *ApJ*, 507, 46
- Shen, K. J. & Bildsten, L. 2009, *ApJ*, 699, 1365
- Shen, K. J., Kasen, D., Miles, B. J., & Townsley, D. M. 2018, *ApJ*, 854, 52
- Shen, K. J. & Moore, K. 2014, *ApJ*, 797, 46
- Shen, K. J. & Schwab, J. 2017, *ApJ*, 834, 180
- Sim, S. A., Röpke, F. K., Hillebrandt, W., et al. 2010, *ApJ*, 714, L52
- Springel, V. 2005, *MNRAS*, 364, 1105
- Stancliffe, R. J. 2010, *MNRAS*, 403, 505
- Taam, R. E. 1980, *ApJ*, 242, 749
- Tauris, T. M. 2015, *MNRAS*, 448, L6
- Tauris, T. M. & Takens, R. J. 1998, *A&A*, 330, 1047
- Toonen, S., Claeys, J. S. W., Mennekens, N., & Ruiter, A. J. 2014, *A&A*, 562, A14
- Townsley, D. M., Miles, B. J., Shen, K. J., & Kasen, D. 2019, *ApJ*, 878, L38
- Vennes, S., Kawka, A., O'Toole, S. J., Németh, P., & Burton, D. 2012, *ApJ*, 759, L25
- Weaver, T. A., Zimmerman, G. B., & Woosley, S. E. 1978, *ApJ*, 225, 1021
- Wheeler, J. C., Lecar, M., & McKee, C. F. 1975, *ApJ*, 200, 145
- Woosley, S. E., Heger, A., & Weaver, T. A. 2002, *Reviews of Modern Physics*, 74, 1015
- Woosley, S. E. & Kasen, D. 2011, *ApJ*, 734, 38
- Woosley, S. E., Taam, R. E., & Weaver, T. A. 1986, *ApJ*, 301, 601
- Yu, Q. & Tremaine, S. 2003, *ApJ*, 599, 1129
- Zeng, Y., Liu, Z.-W., & Han, Z. 2020, *ApJ*, 898, 12
- Zubovas, K., Wynn, G. A., & Gualandris, A. 2013, *ApJ*, 771, 118